IEEE Photonics Journal
An IEEE Photonics Society Publication

Open Access

Higher Order Transport of Intensity Equation Methods: Comparisons and Their Hybrid Application for Noise Adaptive Phase Imaging

Volume 11, Number 3, June 2019

Junbao Hu
Qi Wei
Yan Kong
Zhilong Jiang
Liang Xue
Fei Liu
Dug Young Kim
Cheng Liu
Shouyu Wang

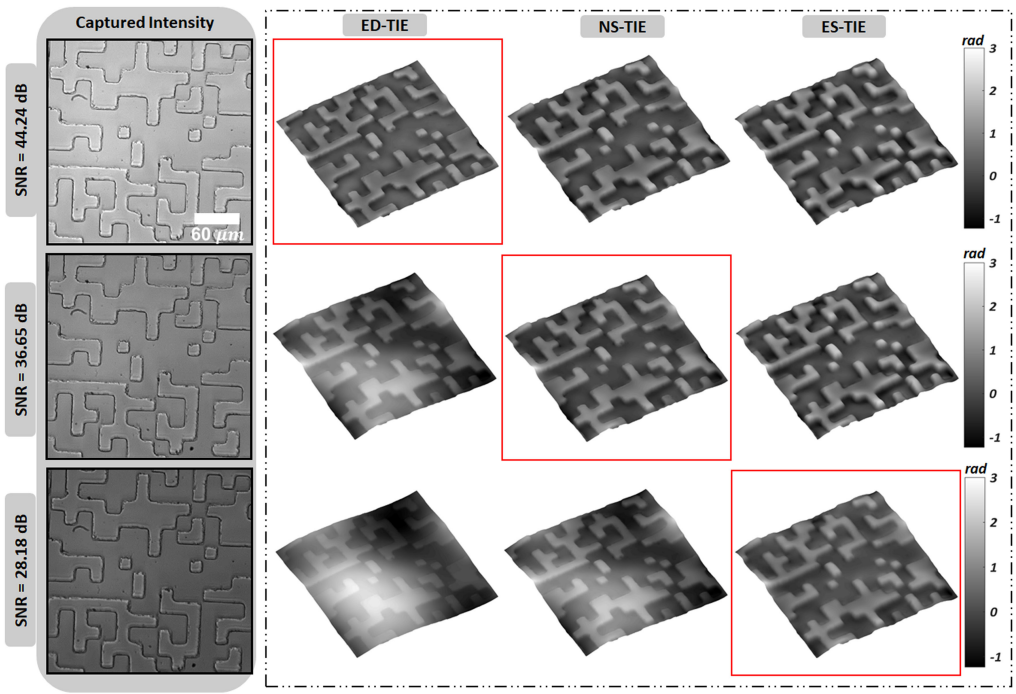

DOI: 10.1109/JPHOT.2019.2919543
1943-0655 © 2019 IEEE

IEEE photonics SOCIETY

IEEE

Higher Order Transport of Intensity Equation Methods: Comparisons and Their Hybrid Application for Noise Adaptive Phase Imaging

Junbao Hu,[1,2] Qi Wei,[1] Yan Kong,[1] Zhilong Jiang,[1] Liang Xue,[3] Fei Liu,[4] Dug Young Kim,[5] Cheng Liu,[1,2] and Shouyu Wang [1,4]

[1]Computational Optics Laboratory, Department of Optoelectric Information Science and Technology, School of Science, Jiangnan University, Wuxi 214122, China
[2]Key Laboratory of High Power Laser and Physics, Shanghai Institute of Optics and Fine Mechanics, Chinese Academy of Sciences, Shanghai 201800, China
[3]College of Electronics and Information Engineering, Shanghai University of Electric Power, Shanghai 200090, China
[4]Single Molecule Nanometry Laboratory, Nanjing Agricultural University, Nanjing 210095, China
[5]Department of Physics, Yonsei University, Seodaemun-gu 120-749, South Korea

DOI:10.1109/JPHOT.2019.2919543

Manuscript received April 10, 2019; revised May 21, 2019; accepted May 23, 2019. Date of publication May 28, 2019; date of current version June 11, 2019. This work was supported by the Natural Science Foundation of China under Grants 61705092, U1730132, and 31870154, in part by the Natural Science Foundation of Jiangsu Province of China under Grants BK20170194, BK20180598, and BE2018709, in part by Shanghai Sailing Program (17YF1407000), and in part by Fundamental Research Funds for the Central Universities (JUSRP51721B). Corresponding authors: Shouyu Wang and Cheng Liu (e-mail: shouyu@jiangnan.edu.cn; chengliu@siom.ac.cn).

Abstract: As a non-interferometric method, the transport of intensity equation (TIE) method suits for quantitative phase imaging with the commercial microscope platform, especially those higher order TIE approaches which can realize precise phase retrieval by eliminating undesired higher order derivatives are widely used. However, these approaches are mostly adopted separately without considering their phase retrieval precision in various noise levels. In this paper, we first compared these classical higher order TIE approaches through theoretical analysis, numerical simulations, and experiments. Then, based on the quantitative comparisons mainly focusing on their phase retrieval accuracy and noise suppression capability, we determine the application scope corresponding to different noise levels of each higher order TIE approach. Finally, in order to deal with different noisy cases, we design the hybrid higher order TIE application, in which the specific higher order TIE approach is selected for phase retrieval according to the precise noise estimation, and the performance of the hybrid higher order TIE application is tested by both the numerical simulations and the experiments, proving it can perform high-quality phase imaging by balancing the tradeoff between the phase retrieval accuracy and the noise influence. The paper not only provides a systematic reference for analysis and comparisons on different higher order TIE approaches, but also proposes the hybrid application for noise adaptive phase imaging, which can be a potential tool in biological observations and medical diagnostics.

Index Terms: Phase imaging, noise in imaging systems, transport of intensity equation.

1. Introduction

Compared to the often used bright/dark field and fluorescent microscopy, quantitative phase microscopy provides a new way for cell and tissue observations. It is able to realize high-contrast imaging without sample staining [1], [2], additionally, the retrieved phase can be adopted for sample detail analysis such as measuring optical thickness and distinguishing sample configurations [3].Therefore, various methods have been proposed to extract quantitative sample phase distributions. Ptychography including spatial domain based ptychographic iterative engine [4], [5] and frequency domain based Fourier ptychographic microscopy [6]–[8] can realize quantitative phase imaging often with extremely large field of view (FoV) and high resolution. However, the massive captures in data collections and the complicated iterations in phase retrieval are both time-consuming. As another widely used phase imaging tool, interference methods composing of quantitative interferometric microscopy [9]–[13] and digital holographic microscopy [14]–[20] can extract sample phases from fringes. But they are easily affected by the external vibrations. Besides, to deal with the phase discontinuities, the required phase unwrapping is often time-consuming. Additionally, since both ptychography and interference approaches rely on coherent sources, and considering the translation stage required in ptychography and the extra reference beam required in interference methods, both these approaches can hardly be integrated with the commercial microscopes, limiting their potential applications in biological and medical fields.

As a non-interferometric method, the transport of intensity equation (TIE) method especially suits for quantitative phase imaging [21]–[39] with the commercial microscope platform, as it can retrieve quantitative sample phases using simple Poisson equation solver [21]–[24] without time-consuming iterations or phase unwrapping. More importantly, TIE method can be implemented with commercial microscopes only with minor modification [40], [41], thus it is a potential phase imaging tool in biological and medical fields. According to phase recovery in TIE, the axial differentiation of the light intensity is required. Teague estimated the axial differentiation from two symmetric defocus images according to the center finite difference method [25]–[27]. Unfortunately, due to the nonlinearity through the focus caused by the diffraction [30], the center finite difference approach corrupts the derivative estimation since it often contains undesired higher order derivatives. In order to correct the nonlinear error, equidistant TIE (ED-TIE) with higher order intensity derivatives was proposed by Waller *et al.* [35], whose core idea is to perform polynomial fitting on intensities along the axial direction, then to extract the first order derivative by removing the higher order terms, but this method is very sensitive to the noise. To inhibit the noise, Soto *et al.* proposed noise suppression TIE (NS-TIE) by ignoring partial higher order terms [36], trying to balance the trade-off between the noise and the linear derivative precision. Besides these equally-spaced tactics, Xue *et al.* proposed TIE methods from multiple intensities captured in unequally-spaced planes to further suppress the noise [38]. Additionally, Zhong *et al.* further pointed out that when the defocus interval satisfies the exponential distribution, the improved exponential spaced TIE (ES-TIE) not only reduces the number of required images, but also performs well noise suppression [39].

Generally, compared to the classical derivative extraction only using two symmetric defocus images, these higher order TIE methods propose linear derivative via nonlinearity error removal, thus always provide sample phase distributions with higher precision. Differently, the ED-TIE method preserves all the nonlinear components of the derivatives through polynomial fitting, therefore, it often has the highest precision in both derivative extraction and phase retrieval, but it is easily affected by the noise. The NS-TIE approach improves the noise suppression by sacrificing partial higher order components as well as the phase retrieval accuracy. Additionally, the ES-TIE method is robust and stable even in higher noise level, but performs relatively lower phase retrieval accuracy. Interestingly, it is reported that these equally spaced strategies can be unified by a type of Savitzky-Golay differential filter with respect to the order of degree and also can be regarded as a special case of it [54]. For instance, ED-TIE and NS-TIE belong to the case where the highest and the lowest order of degree are used in Savitzky-Golay filter, respectively, while ES-TIE representing unequal spacing have no definitive formulation. However, these higher order TIE approaches are mostly used separately for quantitative phase imaging without considering the noise level in

measurements. Since there was no work systematically analyzing these methods or elaborating the most suitable application scopes for these different higher order TIE methods, limiting their practical applications. Though for another perspective, multi-filter TIE phase imaging can also be adopted in order to improve the quantitative phase imaging precision according to different selections of multi-focal image [42]–[44], it is also works well even in unequally spaced interval and partial coherent conditions. However, these approaches only use partial frequency information for phase retrieval, inevitably losing sample information; and they do not consider the noise level as well, for example, only one same filtering is shared under any noise condition, obviously limiting their applications in noise adaptive imaging. In order to achieve high-quality sample phases in different noise levels, this work first provides the quantitative comparisons on these higher order TIE methods mainly focusing on their phase retrieval accuracy and noise suppression capability; next determines the application scope of each higher order TIE method; and finally, designs a hybrid application of these higher order TIE methods, in which different higher order TIE tactic is chosen for optimal phase retrieval according to the estimated noise level. The performance of the hybrid TIE method is certificated by both the numerical simulations and the experiments, proving it can be a promising tool for quantitative phase measurements used in various fields especially in biological observations and medical diagnostics.

In this paper, Section 2 provides the principles of these higher order TIE methods and compares them theoretically; Section 3 and 4 quantitatively compare them numerically and experimentally, respectively, besides, the application scope of each higher order TIE method and their hybrid application are also detailed illustrated in these two sections; and Section 5 sums up this work.

2. Comparisons and Analysis of Higher Order TIE Methods

According to the paraxial approximation, TIE associates the intensity, phase, and its axial intensity derivative illustrated by Eq. (1), in which, λ is the wavelength, $\vec{r}$ is the position vector representing the spatial coordinates, $I(\vec{r})$ stands for the light intensity at the focal plane, $\phi(\vec{r})$ indicates the phase, ∇ is the gradient operator on $\vec{r}$, z denotes the optical axis and $\partial I(\vec{r})/\partial z$ is the axial intensity derivative.

$$-\frac{2\pi}{\lambda}\frac{\partial I(\vec{r})}{\partial z} = \nabla\cdot\left[I(\vec{r})\nabla\phi(\vec{r})\right] \tag{1}$$

In order to extract the phase $\phi(\vec{r})$ by solving the Poisson equation, the classical fast Fourier Transform (*FFT*) based method is adopted [21], [29], thus the quantitative phase can be rapidly calculated according to Eq. (2), where FFT^{-1} indicates inverse *FFT*, $\vec{q}$ indicates the spatial frequency vector.

$$\phi(\vec{r}) = -FFT^{-1}\left\{(\vec{q})^{-2}FFT\left\{\nabla\cdot\left[\left(I(\vec{r})\right)^{-1}\nabla FFT^{-1}\left\{(\vec{q})^{-2}FFT\left\{\frac{2\pi}{\lambda}\frac{\partial I(\vec{r})}{\partial z}\right\}\right\}\right]\right\}\right\} \tag{2}$$

According to the Eq. (2), the axial intensity derivative $\partial I(\vec{r})/\partial z$ is required for phase retrieval. Due to the less captures and simple computation, the classical center finite difference method [21], [22] shown in Eq. (3) is often used, in which Δz is the defocus distance along the z direction.

$$\frac{\partial I(\vec{r})}{\partial z} \approx \frac{I(\vec{r},\Delta z) - I(\vec{r},-\Delta z)}{2\Delta z} \tag{3}$$

Although this approach effectively calculates the axial intensity derivative, the accuracy of the derivative estimation is poor because it often contains undesired higher order derivatives as shown in Eq. (4).

$$\frac{\partial I(\vec{r})}{\partial z} = \frac{I(\vec{r},\Delta z) - I(\vec{r},-\Delta z)}{2\Delta z} - \left[\frac{2\Delta z}{2!}\frac{\partial^2 I(\vec{r})}{\partial z^2} + \frac{(2\Delta z)^2}{3!}\frac{\partial^3 I(\vec{r})}{\partial z^3} + \cdots\right] \tag{4}$$

If the nonlinear error is removed in axial intensity derivative computation, the phase retrieval accuracy can be improved compared to the classical center finite difference method. Since the

higher order intensity derivatives [35]–[39] can be calculated from lower order intensity derivatives, besides, some extremely higher order intensity derivatives are ignored since their values are rather small, Eq. (4) can be rewritten as Eq. (5), which is the superposition of the weighted multi-focal images.

$$\frac{\partial I(\vec{r})}{\partial z} \approx \sum_{i=-n}^{n} \frac{a_i I(\vec{r}, i\Delta z)}{\Delta z} \tag{5}$$

In Eq. (5), a_i stands for the weight, i represents the sequence of the multi-focal images ($i = 0$: in-focus, $i > 0$: over-focus and $i < 0$: under-focus) and n indicates the maximum order of the TIE method. Therefore, in order to obtain the axial intensity derivative free of nonlinear error, a_i should be first determined. Note that reference [43], [52] has demonstrated that the choice of the weight a_i can be used as a trade-off between the amount of noise to be suppressed and the nonlinearity caused by the higher order term of the Taylor expansion. Furthermore, the expression of the weights can be obtained using the Savitzky-Golay differential filter as follows [43], [52], [54]:

$$a_i = \sum_{k=0}^{m} \frac{(2k+1)(2n)^{(k)}}{(2n+k+1)^{(k+1)}} P_k^n(i) P_k^{n,1}(0) \tag{6}$$

In which, $(a)^{(b)}$ is the generalized factorial function, m is the order of degree of the Savitzky-Golay filter, and $P_k^n(t)$ is the Gram polynomials defined as Eq. (7).

$$P_k^{n,s}(t) = \left(\frac{d^s}{dx^s} P_k^n(x) \right)_{x=t} \tag{7}$$

The weights depending on m in Eq. (6) simplify the higher order terms in Taylor expansion, so that some degree of freedom could be retained in the axial intensity derivative for noise suppression. Generally, when using $m = 2n + 1$, the weight formula is simplified to the expression of ED-TIE, and the a_i extraction is calculated by solving the equation listed in Eq. (8) [35].

$$\begin{bmatrix} (-n)^0 & (-n+1)^0 \cdots (n-1)^0 & n^0 \\ (-n)^1 & (-n+1)^1 \cdots (n-1)^1 & n^1 \\ (-n)^2 & (-n+1)^2 \cdots (n-1)^2 & n^2 \\ \vdots & & \ddots \\ (-n)^{2n} & (-n+1)^{2n} \cdots (n-1)^{2n} & n^{2n} \end{bmatrix} \begin{pmatrix} a_{-n} \\ a_{-n+1} \\ a_{-n+2} \\ \vdots \\ a_n \end{pmatrix} = \begin{pmatrix} 0 \\ 1 \\ 0 \\ \vdots \\ 0 \end{pmatrix} \tag{8}$$

Though according to Eq. (8), some extremely higher order intensity derivatives are ignored according to n, the ED-TIE method can still remove as much undesired nonlinear error as possible, it is believed the approach has the highest precision in axial intensity derivative, as well as the phase retrieval. However, since in ED-TIE method, the axial intensity derivative is retrieved from as many higher order intensity derivatives as possible, the noise is easily amplified due to the derivative calculation, thus reducing phase retrieval quality. To reduce the noise influence in phase extraction, Soto proposed a coefficient-dependent finite difference formula [36], in which the restrictions as shown in Eq. (9) are introduced in weight computation.

$$\sum_{i=-n}^{n} a_i = 0, \sum_{i=-n}^{n} a_i \cdot i = 1, \sum_{i=-n}^{n} a_i^2 = \min \tag{9}$$

Therefore, the weights in the NS-TIE method are obtained using the Legendre multiplier as listed in Eq. (10) [36]. Especially, Eq. (10) is exactly the expression of $m = 1$ in Savitzky-Golay differential filter [43].

$$a_i = \frac{3i}{n(n+1)(2n+1)} \tag{10}$$

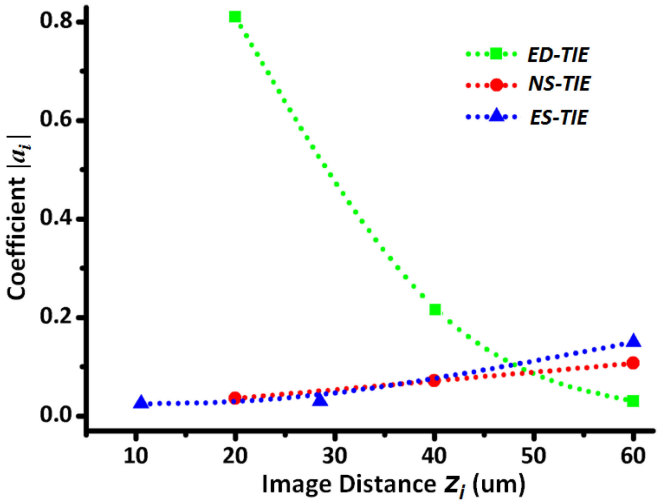

Fig. 1. Weight comparisons of different higher order TIE methods at different defocus distances.

Both the ED-TIE and NS-TIE methods require multi-focal images recorded with equally spaced distances, while in the ES-TIE method, exponential spaced images are captured for phase retrieval [39], in which, the defocus distance z_i is represented in Eq. (11), here α ranging from 0 to 1 and β selected as the power of 2 (such as 2, 4, 8 . . .) are adjusting factors for achieving the exponential spaced distance [39].

$$z_i = \frac{i}{|i|}\alpha\beta^{|i|}\Delta z \tag{11}$$

Moreover, with the extra restriction in Eq. (12), the weight of the ES-TIE is obtained from Eq. (13).

$$\sum_{i=1}^{n}\frac{a_i^2}{(\alpha\beta^i)^2} = \min \tag{12}$$

$$a_i = \frac{i}{|i|}\frac{\alpha\beta^{|i|}}{\sum_{i=1}^{n}(\alpha\beta^{|i|})^2} \tag{13}$$

With the obtained weights, the axial intensity derivative can be computed combining with Eq. (5) via all these three higher order TIE methods (Eqs. (8), (10) and (13), respectively). Considering the phase recovery accuracy of TIE is related to the pixel size, the number of planes, the defocus range and of course, the amount of noise and the weighting coefficient, and among them, we mainly focus on the amount of noise and the weighting coefficient in this paper [42]–[44]. In order to quantitatively compare the weights of these methods, the pixel size of used image is set as 7.4 μm, the defocus range is fixed within $\pm$60 μm, and totally 7 multi-focal images including an in-focus and another 6 defocus images are required. For both the ED-TIE and NS-TIE methods, the defocus recording planes are located at $\pm$20.0, $\pm$40.0 and $\pm$60.0 μm away from the focal plane, while for the ES-TIE method, those are at $\pm$10.5, $\pm$28.5 and $\pm$60.0 μm. Figure 1 illustrates the absolute values of weights at different defocus distances (here, we only show the over-focus case, the under-focus case is the same). It is obvious that in ED-TIE method, the weights close to the focal plane are much higher than those far from the focal plane, indicating that the retrieved axial intensity derivative often preserves more details, while it is easily influenced by the noise. While in the ES-TIE method, the weight distribution is opposite to that of the ED-TIE method, indicating that the detail preservation is lower than the ED-TIE method, but it is robust in severely noisy conditions. Considering the weight distribution of the NS-TIE is between the ED-TIE and the ES-TIE methods, it balances the trade-off between the phase retrieval accuracy and the noise influence. In order to

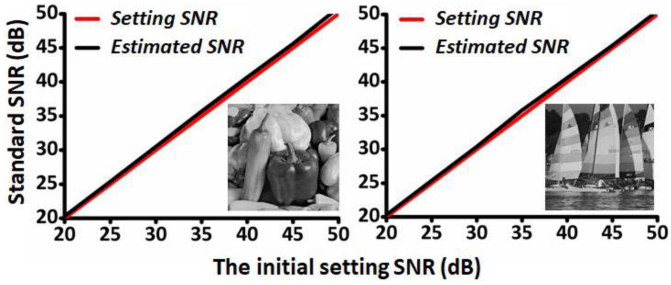

Fig. 2. Numerical certification on the mean-value filter method.

certificate the conclusion obtained from the theoretical analysis, and to numerically compare these classical higher order TIE methods, the numerical simulation was implemented with the quantitative evaluation of their phase retrieval performance.

3. Performance Characterization of Higher Order TIE by Simulations

According to the theoretical analysis, with the same defocus range and the number of the multi-focal image captures, the ED-TIE method has the highest phase retrieval accuracy, but it is easily influenced by the noise; the ES-TIE has the best noise suppression capability, however its phase retrieval accuracy is a little lower. In order to further evaluate their phase retrieval accuracy and noise suppression capability, numerical simulations are provided here. Since the robustness of these methods in noisy cases should be quantitatively compared, an appropriate signal to noise ratio (SNR) estimation method should be used to evaluate the noise level from the captured images. Generally, the process of light shooting into photosensitive region of the image recorder to generate signal charge can be treated as a random process that occurs independently, uniformly, and continuously [49], [50]. Considering a CCD camera for image recording used in our self-built experimental system is mainly affected by thermal and exposure noise, and thus the white Gaussian noise was used in the numerical computation to stimulate the random process, which is similar as those in reported works [42], [43], [51]. Here, the mean-value filter method [45], [46] was applied, in which, multiple images were first captured, and then their average value was treated as the noise-free image, finally the SNR could be estimated. Figure 2 displays the quantitative comparisons between the setting noise and the estimated noise, which shows that the estimated SNRs are rather close to the setting ones, proving the effectiveness of the mean-value filter method. Since the estimated SNR can accurately reflect the noise level, in the following numerical simulations, the listed SNR values were all estimated via this mean-value filter method.

After the certification of the SNR estimation, the numerical simulations were then provided: the setting amplitude and phase are listed in Figure 3(A) and 3(B), respectively. The wavelength was set as 633 nm, the pixel size of the image recorder was 7.4 μm and the total number of pixels was 512 $\times$ 512, all according to the experimental setup. Using the angular spectrum method [47], [48] for numerical wavefront propagation, multi-focal images can be computed as shown in Figure 3(C). Before introducing noises, the phase retrieval accuracy of the ED-TIE, the NS-TIE and the ES-TIE approaches was first tested. Figure 3(D) lists the recovered phases via these methods. According to the quantitative RMSE evaluation, the RMSE values corresponding to these methods are 0.0632, 0.0823, 0.1297 respectively, indicating that the ED-TIE has the highest phase retrieval accuracy, while the accuracy of the NS-TIE and ES-TIE methods is a little lower. However, it is worth noting that these rather small RMSE values prove that all these methods can extract the satisfied sample phases with rather high precision.

Next, the phase retrieval accuracy of these higher order TIE methods was tested in different noisy conditions. Figure 4(A) lists three in-focus intensities with different estimated SNRs as 44.78, 34.49 and 24.82 dB, representing the low, moderate and severe noise levels, respectively. All these higher

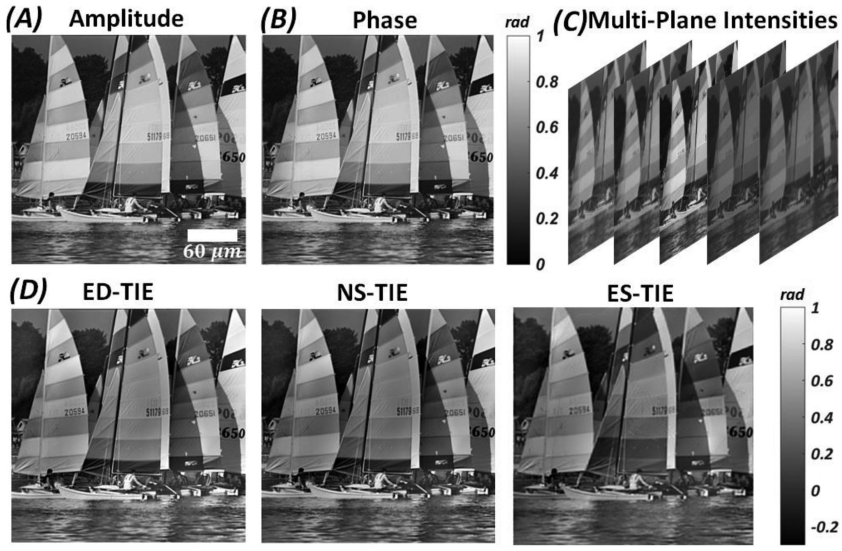

Fig. 3. (A) amplitude and (B) phase distributions originally set in the simulation; (C) numerically propagated multi-focal intensities; (D) retrieved phases using the ED-TIE, the NS-TIE and the ES-TIE methods, respectively. The white bar in (A) indicates 60 μm.

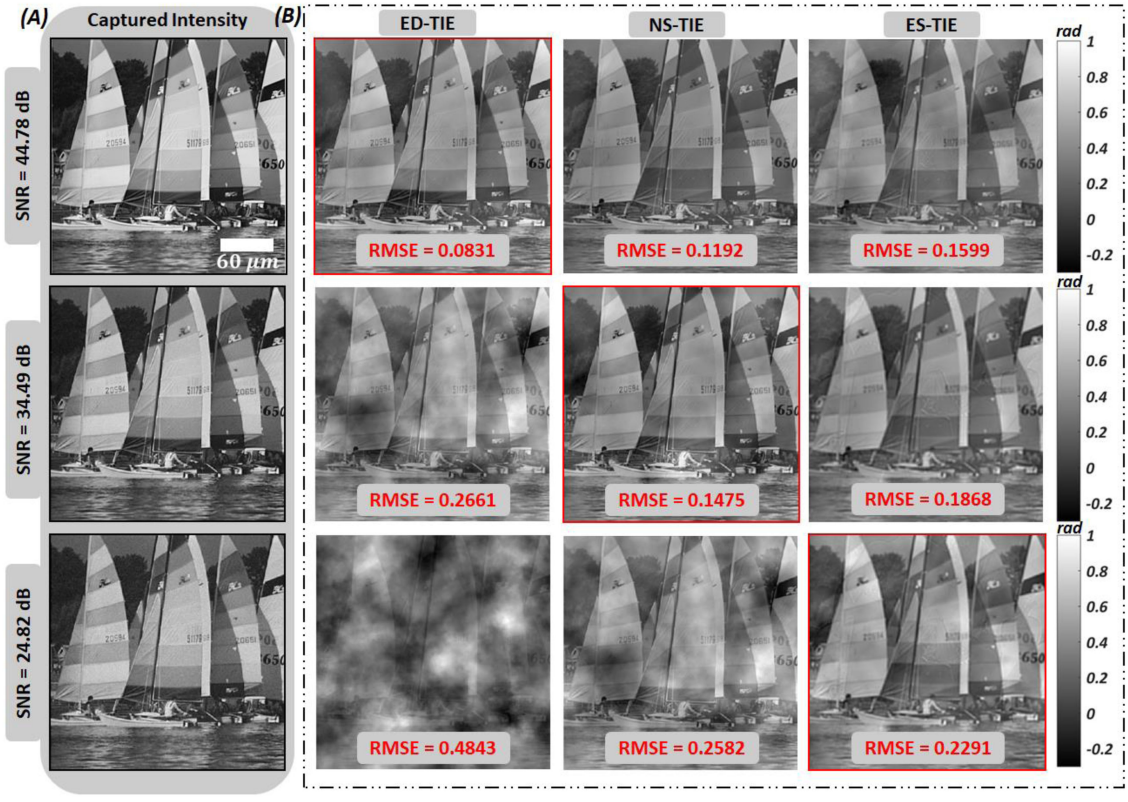

Fig. 4. Simulated phase recovery results. (A) the in-focus intensities with different SNRs; (B) the retrieved phases using the ED-TIE, the NS-TIE and the ES-TIE methods, respectively. The red box marks the appropriate higher order TIE method and the values listed are the estimated RMSE values. The white bar in (A) indicates 60 μm.

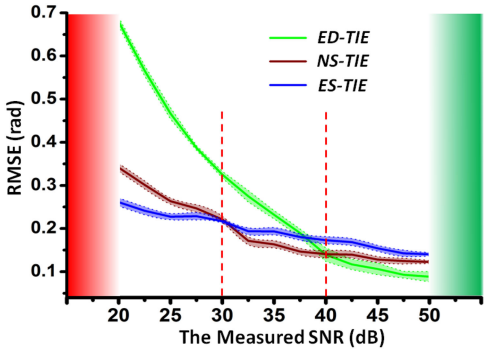

Fig. 5. Quantitative determination on the application scopes of different higher order TIE methods in different noise conditions.

order TIE methods were adopted for phase retrieval in various noisy conditions as shown in Figure 4(B). The required defocus planes were at 20.0, 40.0 and 60.0 μm for both the ED-TIE and the NS-TIE methods, while those were at 10.5, 28.5 and 60.0 μm for the ES-TIE method, illustrating that totally seven multi-focal images were within the maximum defocus range of $\pm$60 μm. When the SNR was 44.78 dB, all these methods can provide high-quality phases, however, evaluated by the RMSE, the ED-TIE method has the highest precision, while that of the NS-TIE and the ES-TIE is lower. When the SNR decreased to 34.49 dB, the ED-TIE method became invalid due to the artifact generated by the noise, while the NS-TIE and the ES-TIE methods still worked well. Considering the phase retrieval accuracy evaluated by RMSE, NS-TIE has the higher phase retrieval accuracy in moderate noise conditions. While when the SNR was 24.82 dB indicating there was severe noise in the captured multi-focal images, artifact occurred in the phase distributions retrieved by both the ED-TIE and the NS-TIE methods, only the ES-TIE approach could provide satisfied phase imaging with a relatively low RMSE value. According to the results shown in Figure 4, it shows that the ED-TIE method fits for low noise case, though it often has the highest phase retrieval accuracy, and it is easily influenced by the noise; the NS-TIE method is appropriate for moderate noise conditions, as it well balances the trade-off between the phase retrieval accuracy and the noise influence; the ES-TIE method is the only choice in dealing with the severely noisy cases, though its phase retrieval accuracy is not the highest one. It is believed these higher order TIE methods have their own application scopes in different noise conditions.

In order to determine their corresponding application scopes, their phase retrieval performances with various SNRs from 20 dB to 50 dB were quantitatively tested. For a specific SNR, totally 10 computations with the whole noisy multi-focal image generation and phase retrieval processing were implemented, and the corresponding average (center point) and standard deviation (line width) of the RMSE values were shown in Figure 5. According to the quantitatively evaluated RMSE, when the SNR is higher than 40 dB, the ED-TIE method should be used to pursue the high phase retrieval precision; when the SNR is between 30 dB and 40 dB, the NS-TIE approach is preferred; and when the SNR is below 30 dB, only the ES-TIE method can be used to extract the sample phase to avoid the artifact caused by the noise.

The proposed numerical simulation not only quantitatively compared the phase accuracy and noise suppression capability, but also determined the application scope for each higher order TIE method. According to the numerical simulation, since these higher order TIE methods have their own corresponding application scopes, their hybrid adoption can effectively expand the application scope in various SNR conditions, which means an appropriate higher order TIE method can be chosen for phase retrieval with high phase retrieval accuracy while avoiding the artifact induced by noise. In the following experiments, not only the comparisons among these three higher order TIE methods were provided, their hybrid application was also tested to prove the potentiality in noise adaptive quantitative phase microscopy.

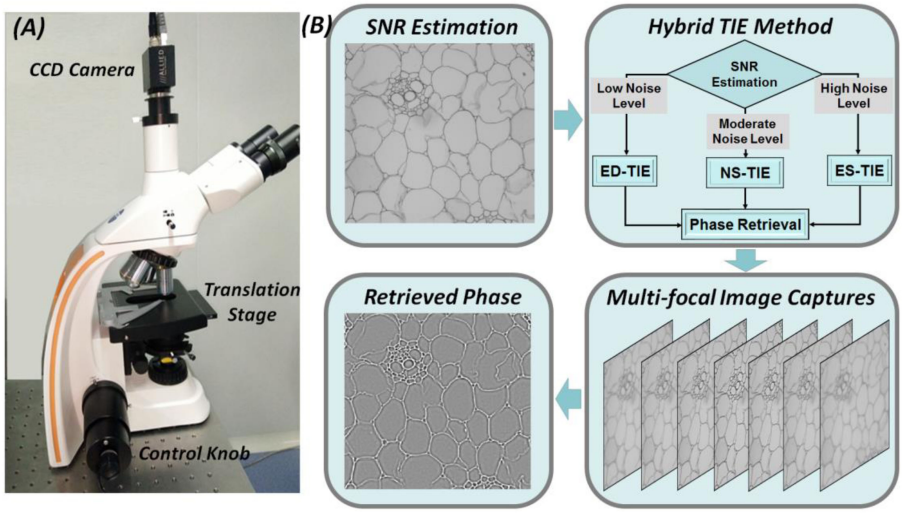

Fig. 6. (A) Experimental setup and (B) flow-chart of the hybrid higher order TIE approach.

4. Practical Applications of Hybrid Higher Order TIE by Experiments

The previous numerical simulations indicate that the ED-TIE, the NS-TIE and the ES-TIE methods respectively suit for low, moderate and severe noise cases, therefore, considering the trade-off between the phase retrieval accuracy and the noise influence, their hybrid application becomes an appropriate choice for high-quality phase imaging in various SNR conditions. Next, experiments with different samples as standard phase steps and biological samples were proposed, not only to provide experimental comparisons among these higher order TIE methods, but also to test the performance of their hybrid application. Figure 6(A) shows the experimental setup based on a commercial upright microscope (ML-32, Mshot, China). The microscope was modulated in Kohler illumination and the condenser aperture was set as $\sim$40% of the objective aperture to ensure the partial spatial coherence. Besides, an interference filter with the central wavelength of 633 nm and the full width at half maximum of 10 nm (Daheng Optics, China) was used to improve the temporal coherence, since the high illumination coherence can guarantee accurate phase retrieval when using TIE methods [21], [24], [30]. A 10$\times$ objective was used for sample magnification. The sample position could be scanned along the optical axis using a motorized sample stage (Mshot MS-300, China) with the step of 0.5 μm, and the multi-focal images were recorded by a CCD camera (Prosilica GC780, Allied Vision, Germany). In the experiments, the SNR was easily adjusted by changing the exposure time [30], and the SNR could be precisely estimated by the mean-value filtering method previously proved by the numerical simulations. Besides, the total number of pixels was adopted as 512 $\times$ 512, which is consistent with the simulation. According to the flow chart of the hybrid higher order TIE approach shown in Figure 6(B), multiple images are first captured to evaluate the SNR (here we captured 12 images for SNR evaluation). Next, based on the estimated SNR, one of the higher order TIE methods is chosen for phase retrieval, and accordingly, multi-focal images at different recording planes need to be captured by shifting the motorized sample stage. Finally, quantitative phases can be computed from the linear intensity derivative using the classical Fourier transform based method.

First, a random phase plate (fabricated by Shanghai Institute of Optics and Fine Mechanics, Chinese Academy of Sciences) acting as the standard sample was measured for both imaging system certification and the hybrid TIE method test. There are only two phase values with the phase difference of π when the illumination wavelength is 633 nm. Figure 7 shows the results of the random phase plate including both the in-focus images captured with different exposure times as 0.15, 0.11, 0.07 s and the retrieved phases via different higher order TIE methods. In the experiments, totally 7 multi-focal images were captured including an in-focus image and another

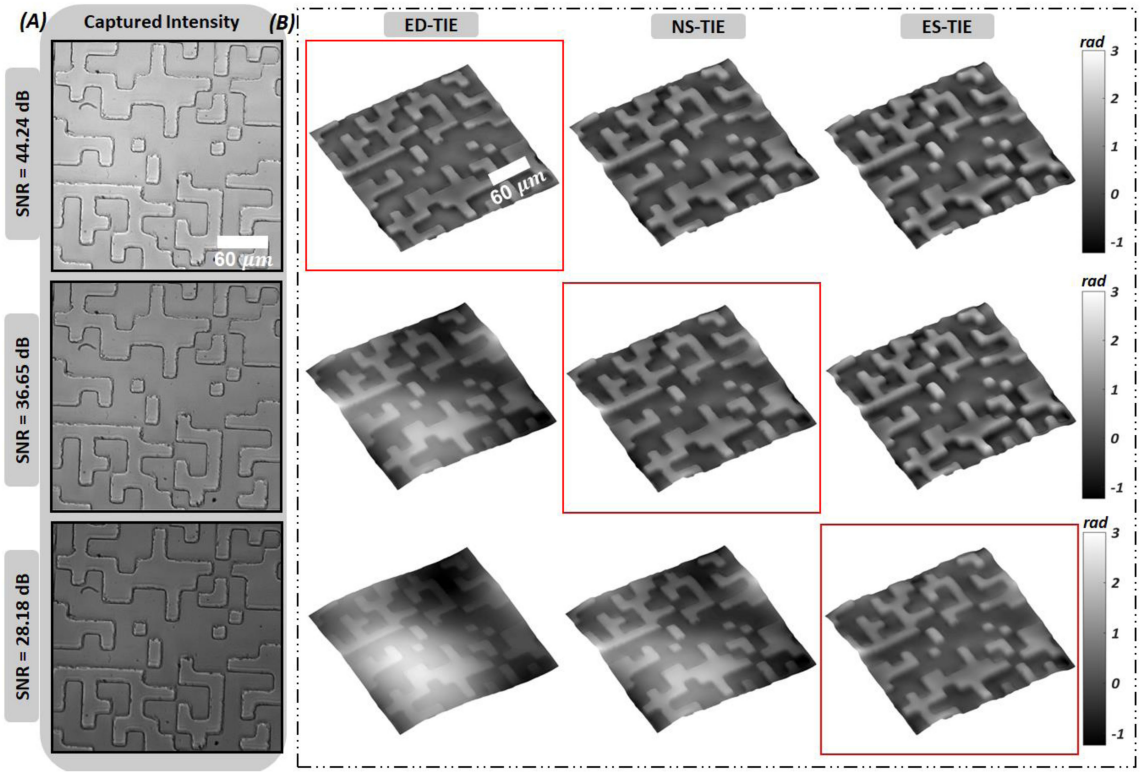

Fig. 7. Experimental results of random phase plate. (A) in-focus images captured with the different exposure times as 0.15, 0.11 and 0.07 s with the estimated SNRs as 44.24 dB, 36.65 dB and 28.18 dB, respectively. (B) phase recovery using different higher order TIE methods in various SNR conditions, the white bar in (A) indicates 60 μm. The red box marks the appropriate higher order TIE method.

six defocus ones, for both the ED-TIE and the NS-TIE methods, the defocus distances were $\pm$20.0, $\pm$40.0, and $\pm$60.0 μm; while for the ES-TIE method, the defocus distances were $\pm$10.5, $\pm$28.5, and $\pm$60.0 μm, both were the same as those in numerical simulations. With the adjustment of the exposure time, different SNRs were estimated as 44.24, 36.65 and 28.18 dB, representing the low, moderate and severe noise conditions, respectively. In comparison, phase recovery by these methods was listed in Figure 7(B), when the noise level was low as the estimated SNR was 44.24 dB higher than 40 dB, the ED-TIE method was preferred for phase retrieval. Besides, all these higher order TIE methods can provide high-quality phase retrievals with the phase step of $\sim\pi$, proving the high precision of the imaging system. As the noise level increased with a SNR of 36.65 dB, the ED-TIE method was invalid due to the noise generated artifact, and the NS-TIE approach was selected in the moderate noisy condition. While in the severely noisy cases, only the ES-TIE method could provide the satisfied result. With the random phase plate, the accuracy of the imaging system was certificated since the retrieved phase distribution indicated the obvious $\sim\pi$ difference. Additionally, based on the comparative phase retrieval results in Figure 7(B), it shows that the ED-TIE, the NS-TIE and the ES-TIE methods suit for the high, moderate and low SNR cases, respectively, indicating that their hybrid application can expand the application scopes in different noise cases.

Besides, commercial smears as plant rhizome cross cutting and epidermis of broad bean (both brought from Keda Biological Sample Company, China) were chosen as the testing samples. Figure 8 shows the experimental results of the plant rhizome cross cutting, Figure 8(A) lists the in-focus images with different exposure times as 0.12, 0.08 and 0.04 s respectively, and their SNRs were estimated as 45.72 dB, 36.34 dB and 27.53 dB according to the mean-value filtering method. In order to achieve high-quality phase imaging, when the SNR was estimated as 45.72 dB,

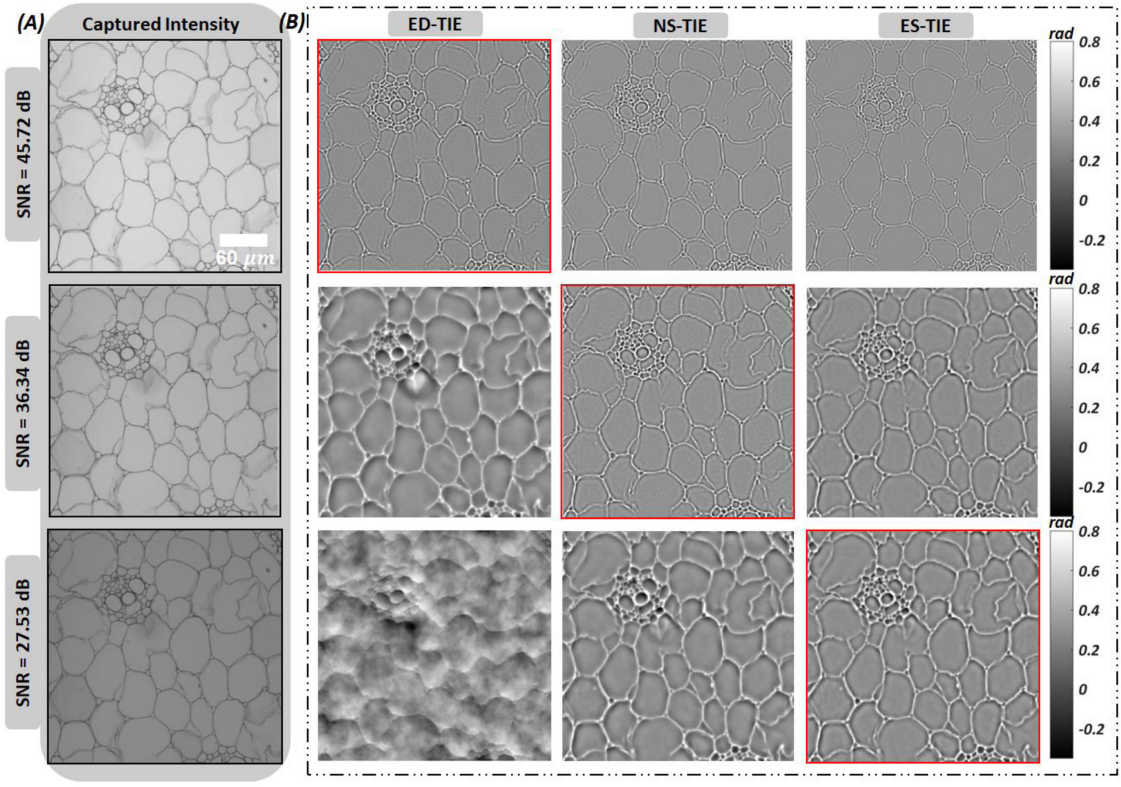

Fig. 8. Experimental results of plant rhizome cross cutting. (A) in-focus images captured with the different exposure times as 0.12, 0.08 and 0.04 s with the estimated SNRs as 45.72 dB, 36.34 dB and 27.53 dB, respectively. (B) phase recovery using different higher order TIE methods in various SNR conditions, the white bar in (A) indicates 60 μm. The red box marks the appropriate higher order TIE method.

phase should be computed using the ED-TIE method, while when the SNRs were 36.34 dB and 27.53 dB, the NS-TIE and the ES-TIE methods should be adopted, respectively. In order to test the performance of their hybrid application, Figure 8(B) lists the phase recovery using all these higher order TIE methods in various SNR conditions. In the experiments, still 7 multi-focal images were captured with the coincidence recording planes in the numerical simulations. In the high SNR case of 45.72 dB, all these three methods can provide high-quality phase recovery, however, the phase image obtained by the ED-TIE method often has the highest accuracy since it removes all the nonlinear derivatives. When the noise increased as the SNR was 36.34 dB, phase retrieved by the ED-TIE method was easily influenced by the noise, while the NS-TIE approach especially suits for this case, though in the procedure of linear intensity derivative solution, partial higher order information was ignored to suppress the noise. When the SNR was decreased to 27.53 dB, both the ED-TIE and the NS-TIE methods were invalid, while the ES-TIE approach could still provide satisfied quantitative phase imaging, though sacrificing partial accuracy indicated in the numerical simulations. The experimental results of the plant rhizome cross cutting not only provide the experimental comparisons on the retrieved phases via different higher order TIE methods in different noise levels, but also prove that the hybrid higher order TIE method can obtain high-quality phase imaging in various SNR cases with the help of the noise estimation.

Figure 9 exhibits the results of another sample as the epidermis of broad bean, Figure 9(A) lists three in-focus intensities captured with different exposure times as 0.12, 0.08 and 0.04 s with the estimated SNRs as 43.89 dB, 36.21 dB and 27.74 dB, respectively. Similar to the experiments shown in Figure 7, 8 and numerical simulations, still 7 multi-focal images were captured within the defocus range of $\pm$60.0 μm. According to the hybrid higher order TIE method, in the case of SNR

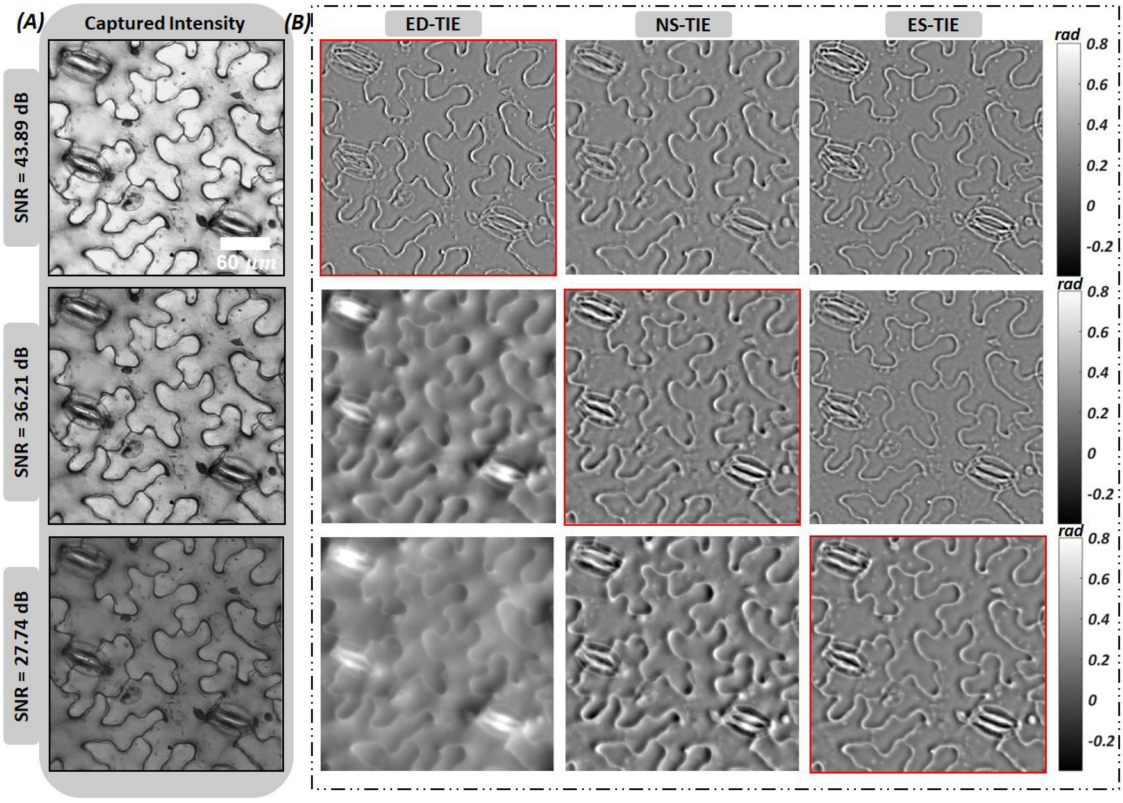

Fig. 9. Experimental results of broad bean epidermis. (A) in-focus images captured with the different exposure times as 0.12, 0.08 and 0.04 s with the estimated SNRs as 43.89 dB, 36.21 dB and 27.74 dB, respectively. (B) phase recovery using different higher order TIE methods in various SNR conditions, the white bar in (A) indicates 60 μm. The red box marks the appropriate higher order TIE method.

as ∼44 dB, the ED-TIE method was preferred; when the SNR decreased to ∼36 dB, the NS-TIE approach was appropriate to balance the noise and the phase retrieval accuracy; and when the SNR was ∼28 dB, only the ES-TIE method provided the satisfied result, these optimal retrieved phases are marked in Figure 9(B). Moreover, according to the experimental comparisons shown in Figure 9(B), it is believed the hybrid higher order TIE method worked well in various SNR conditions.

Based on the comparative results from both the numerical simulations shown in Figure 4 and the experiments shown in Figures 7, 8 and 9, it shows that these higher order TIE methods have different application scopes in different noise levels. Therefore, in order to deal with different noise cases, their hybrid application is proposed, considering the advantages as adaptive noise reduction and high-quality phase retrieval proved by both the numerical simulations and experiments, their hybrid application can be potentially used in biomedical observation and measurements in various noise conditions.

5. Conclusions

In this paper, we quantitatively compared these classical higher order TIE methods including the ED-TIE, the NS-TIE and the ES-TIE approaches through theoretical analysis, numerical simulations and practical experiments. It indicates that the ED-TIE approach has the highest phase retrieval precision, but it is easily influenced by the noise; though the phase retrieval accuracy of the ES-TIE approach is the lowest among them, it is the most robust in severe noise existing conditions. Therefore, in order to obtain high-quality sample phase imaging in various noise conditions, we designed the hybrid application of these higher order TIE methods. Proved by both numerical

simulations and practical experiments, compared to the separate use of these higher order TIE methods, their hybrid application can provide phase recovery with higher quality by considering both the phase retrieval accuracy and noise suppression, indicating their hybrid application is potential in biological observations and medical diagnostics as a noise adaptive quantitative phase imaging tool. However, the hybrid application presented in this paper mainly concentrates on existing three representative methods through comparisons and analysis, how to construct a new noise adaptive model integrating all the higher order methods to realize adaptively noise-orientated phase imaging will be our next work.

Acknowledgment

Competing Interests: Authors have declared that no competing interests exist.

References

[1] T. Kim, R. Zhou, L. L. Goddard, and G. Popescu, "Breakthroughs in photonics 2013: quantitative phase imaging: Metrology meets biology," *IEEE Photon. J.*, vol. 6, no. 2, Apr. 2014, Art. no. 0700909.
[2] Y. Jo *et al.*, "Quantitative phase imaging and artificial intelligence: A review," *IEEE J. Sel. Topic Quantum Electron.*, vol. 25, no. 1, pp. 1–14, Jan./Feb. 2019.
[3] G. Popescu, T. Ikeda, R. R. Dasari, and M. S. Feld, "Diffraction phase microscopy for quantifying cell structure and dynamics," *Opt. Lett.*, vol. 31, no. 6, pp. 775–778, 2006.
[4] J. M. Rodenburg and H. M. L. Faulkner, "A phase retrieval algorithm for shifting illumination," *Appl. Phys. Lett.*, vol. 85, no. 20, pp. 4795–4797, 2004.
[5] F. Hüe, J. M. Rodenburg, A. M. Maiden, F. Sweeney, and P. A. Midgley, "Wave-front phase retrieval in transmission electron microscopy via ptychography," *Phys. Rev. B*, vol. 82, no. 12, 2010. Art. no. 121415.
[6] G. Zheng, R. Horstmeyer, and C. Yang, "Wide-field, high-resolution Fourier ptychographic microscopy," *Nature Photon.*, vol. 7, no. 9, pp. 739–746, 2013.
[7] G. Zheng, "Breakthroughs in photonics 2013: Fourier ptychographic imaging," *IEEE Photon. J.*, vol. 6, no. 2, Apr. 2014, Art. no. 0701207.
[8] Y. Zhang, W. Jiang, and Q. Dai, "Nonlinear optimization approach for Fourier ptychographic microscopy," *Opt. Exp.*, vol. 23, no. 26, pp. 33822–33835, 2015.
[9] S. Chen, T. Xu, J. Zhang, X. Wang, and Y. Zhang, "Optimized denoising method for fourier ptychographic microscopy based on wirtinger flow," *IEEE Photon. J.*, vol. 11, no. 1, Feb. 2019, Art. no. 3900214.
[10] A. Nativ and N. T. Shaked, "Compact interferometric module for full-field interferometric phase microscopy with low spatial coherence illumination," *Opt. Lett.*, vol. 42, no. 8, pp. 1492–1495, 2017.
[11] J. Xu *et al.*, "Accelerating wavefront-sensing-based autofocusing using pixel reduction in spatial and frequency domains," *Appl. Opt.*, vol. 58, no. 11, pp. 3003–3012, 2019.
[12] L. Xue, J. Vargas, S. Wang, Z. Li, and F. Liu, "Quantitative interferometric microscopy cytometer based on regularized optical flow algorithm," *Opt. Commun.*, vol. 350, no. 8, pp. 222–229, 2015.
[13] S. Shin, K. Kim, K. Lee, S. Lee, and Y. Park, "Effects of spatiotemporal coherence on interferometric microscopy," *Opt. Exp.*, vol. 25, no. 7, pp. 8085–8097, 2017.
[14] V. Bianco, P. Memmolo, M. Paturzo, A. Finizio, B. Javidi, and P. Ferraro, "Quasi noise-free digital holography," *Light Sci. Appl.*, vol. 5, no. 9, 2016. Art. no. e16142.
[15] A. Finizio *et al.*, "An automatic method for assembling a large synthetic aperture digital hologram," *Opt. Exp.*, vol. 20, no. 5, pp. 4830–4839, 2012.
[16] W. Osten, T. Baumbach, and W. Jüptner, "Comparative digital holography," *Opt. Lett.*, vol. 27, no. 20, pp. 1764–1767, 2002.
[17] J. Di, Y. Li, K. Wang, and J. Zhao, "Quantitative and dynamic phase imaging of biological cells by the use of the digital holographic microscopy based on a beam displacer unit," *IEEE Photon. J.*, vol. 10, no. 4, Aug. 2018, Art. no. 6900510.
[18] L. Wang, C. Liu, and J. M. Rodenburg, Possibility of high-resolution ptychographic iterative imaging with low energy electrons: Dynamical calculations, *Microscopy*, vol. 62, no. 2, pp. 105–110, 2015.
[19] D. Blinder, C. Schretter, H. Ottevaere, A. Munteanu, and P. Schelkens, "Unitary transforms using time-frequency warping for digital holograms of deep scenes," *IEEE Trans. Comput. Imag.*, vol. 4, no. 2, pp. 206–218, Jun. 2018.
[20] I. Masatoshi, "Radiometric temperature measurement by incoherent digital holography," *Appl. Opt.*, vol. 58, no. 5, pp. A82–A89, 2019.
[21] T. E. Gureyev, A. Roberts, and K. A. Nugent, "Partially coherent fields, the transport-of-intensity equation, and phase uniqueness," *J. Opt. Soc. America A*, vol. 12, no. 4, pp. 1942–1946, 1995.
[22] T. E. Gureyev, A. Roberts, and K. A. Nugent, Phase retrieval with the transport-of-intensity equation: matrix solution with use of Zernike polynomials, *J. Opt. Soc. Amrica A*, vol. 12, no. 4, pp. 1932–1942, 1995.
[23] T. E. Gureyev and K. A. Nugent, "Rapid quantitative phase imaging using the transport of intensity equation," *Opt. Commun.*, vol. 133, no. 6, pp. 339–346, 1997.
[24] T. E. Gureyev and Y. I. Nesterets, "Partially coherent contrast-transfer-function approximation," *J. Opt. Soc. America A*, vol. 33, no. 4, pp. 464–474, 2016.
[25] M. R. Teague, "Deterministic phase retrieval: a Green's function solution," *J. Opt. Soc. America A*, vol. 73, no. 11, pp. 1434–1441, 1983.

[26] M. R. Teague, "Irradiance moments: their propagation and use for unique retrieval of phase," *J. Opt. Soc. America A*, vol. 72, no. 9, pp. 1199–1209, 1982.
[27] M. R. Teague, "Image formation in terms of the transport equation," *J. Opt. Soc. America A*, vol. 2, no. 11, pp. 2019–2026, 1985.
[28] C. Roddier and F. Roddier, "Wave-front reconstruction from defocused images and the testing of ground-based optical telescopes," *J. Opt. Soc. America A*, vol. 10, no. 11, pp. 2277–2287, 1993.
[29] D. Paganin and K. A. Nugent, "Noninterferometric phase imaging with partially coherent light," *Phys. Rev. Lett.*, vol. 80, no. 12, pp. 2586–2589, 1998.
[30] D. Paganin, A. Barty, P. J. Mcmahon, and K. A. Nugent, "Quantitative phase-amplitude microscopy. III. The effects of noise," *J. Microsc.*, vol. 214, no. 1, pp. 51–61, 2004.
[31] E. Alberto, J. Müller, M. Huang, and C. T. Koch, "Multi-focus TIE algorithm including partial spatial coherence and overlapping filters." *Opt. Exp.*, vol. 26, no. 9, pp. 11819–11833, 2018.
[32] Y. Shan *et al.*, "Measurements on ATP induced cellular fluctuations using real-time dual view transport of intensity phase microscopy," *Biomed. Opt. Exp.*, vol. 10, no. 5, pp. 2337–2354, 2019.
[33] J. Hu *et al.*, "Adaptive dual-exposure fusion-based transport of intensity phase microscopy," *Appl. Opt.*, vol. 57, no. 25, pp. 7249–7258, 2018.
[34] S. S. Kou, L. Waller, G. Barbastathis, and C. J. R. Sheppard, "Transport-of-intensity approach to differential interference contrast (TI-DIC) microscopy for quantitative phase imaging," *Opt. Lett.*, vol. 35, no. 3, pp. 447–449, 2010.
[35] L. Waller, L. Tian, and G. Barbastathis, "Transport of Intensity phase-amplitude imaging with higher order intensity derivatives," *Opt. Exp.*, vol. 18, no. 12, pp. 12552–12561, 2010.
[36] M. Soto and E. Acosta, "Improved phase imaging from intensity measurements in multiple planes," *Appl. Opt.*, vol. 46, no. 33, pp. 7978–7981, 2007.
[37] A. M. Zysk, R. W. Schoonover, P. S. Carney, and M. A. Anastasio, "Transport of intensity and spectrum for partially coherent fields," *Opt. Lett.*, vol. 35, no. 13, pp. 2239–2243, 2010.
[38] S. Zheng, B. Xue, W. Xue, X. Bai, and F. Zhou, "Transport of intensity phase imaging from multiple noisy intensities measured in unequally-spaced planes," *Opt. Exp.*, vol. 19, no. 21, pp. 972–985, 2011.
[39] J. Zhong, R. A. Claus, J. Dauwels, L. Tian, and L. Waller, "Transport of intensity phase imaging by intensity spectrum fitting of exponentially spaced defocus planes," *Opt. Exp.*, vol. 22, no. 9, pp. 10661–10670, 2014.
[40] X. Meng *et al.*, "Smartphone based hand-held quantitative phase microscope using the transport of intensity equation method," *Lab Chip*, vol. 17, no. 1, pp. 104–109, 2017.
[41] J. Hu *et al.*, "Numerical tilting compensation in microscopy based on wavefront sensing using transport of intensity equation method," *J. Opt.*, vol. 20, no. 3, 2018, Art. no. 035301.
[42] M. H. Jenkins, J. M. Long, and T. K. Gaylord, "Multifilter phase imaging with partially coherent light," *Appl. Opt.*, vol. 53, no. 16, pp. D29–D39, 2014.
[43] J. Martinez-Carranza, K. Falaggis, and T. Kozacki, "Optimum plane selection for transport of intensity-equation-based solvers," *Appl. Opt.*, vol. 53, no. 30, pp. 7050–7058, 2014.
[44] J. Martinez-Carranza, K. Falaggis, and T. Kozacki, "Multi-filter transport of intensity equation solver with equalized noise sensitivity," *Opt. Exp.*, vol. 23, no. 18, pp. 23092–23107, 2015.
[45] J. Bourgain and C. Demeter, "Mean value estimates for Weyl sums in two dimensions," *J. London Math. Soc.*, vol. 94, no. 3, pp. 814–838, 2016.
[46] T. D. Wooley, "Multigrade efficient congruencing and Vinogradov's mean value theorem," *Proc. London Math. Soc.*, vol. 111, no. 3, pp. 519–560, 2015.
[47] M. E. Schafer and P. A. Lewin, "Transducer characterization using the angular spectrum method," *J. Opt. Soc. America A*, vol. 25, no. 5, pp. 152–161, 1989.
[48] K. Matsushima and T. Shimobaba, "Band-limited angular spectrum method for numerical simulation of free-space propagation in far and near fields," *Opt. Exp.*, vol. 17, no. 3, pp. 19662–19671, 2009.
[49] G. E. Healey and R. Kondepudy, "Radiometric CCD camera calibration and noise estimation," *IEEE Trans. Pattern Anal.Mach. Intell.*, vol. 16, no. 3, pp. 267–276, Mar. 1994.
[50] J. Hynecek, "Theoretical analysis and optimization of CDS signal processing method for CCD image sensors," *IEEE Trans. Electron. Device*, vol. 39, no. 11, pp. 2497–2507, Nov. 1992.
[51] K. Falaggis, T. Kozacki, and M. Kujawinska, "Hybrid single-beam reconstruction technique for slow and fast varying wave fields," *Opt. Lett.*, vol. 40, no. 11, pp. 2509–2512, 2015.
[52] A. Savitzky and M. J. Golay, "Smoothing and differentiation of data by simplified least squares procedures," *Anal. Chem.*, vol. 36, no. 5, pp. 1627–1639, 1964.
[53] P. A. Gorry, "General least-squares smoothing and differentiation of nonuniformly spaced data by the convolution method," *Anal. Chem.*, vol. 63, no. 5, pp. 534–536, 1991.
[54] C. Zuo, Q. Chen, Y. Yu, and A. Asundi, "Transport-of-intensity phase imaging using Savitzky-Golay differentiation filter-theory and applications," *Opt. Exp.*, vol. 21, no. 5, pp. 5346–5362, 2013.